

MICROSTRUCTURE AND PROPERTIES OF BIOCOMPATIBLE Mg-Ca-Zn-Mn ALLOY

¹Michal KOPELANT, ¹Monika LOSERTO VÁ, ²Vojtěch HAVLAS, ¹Kateřina KONEČNÁ,
¹Petr LICHÝ, ¹Miroslav GREGER, ³Eva JABLONSKÁ, ¹Alžběta ĎURÍKOVÁ

¹*VSB - Technical University of Ostrava, Faculty of Materials Science and Technology Ostrava, Czech Republic, EU, michal.kopelent@vsb.cz*

²*Charles University, Second Faculty of Medicine, Prague, Czech Republic, EU,*

³*University of Chemistry and Technology, Prague, Faculty of Food and Biochemical Technology, Czech Republic, EU,*

<https://doi.org/10.37904/metal.2022.4514>

Abstract

Nowadays, implants are predominantly made of metallic materials that have two main problems. The first resides in the modulus of elasticity being higher than the one of the human bone (10-20 GPa), resulting in stress shielding and subsequent implant failure. The second problem is the toxicity of some constitution elements of implant materials, which can lead to inflammation of the surrounding tissue due to the release of cytotoxic ions during the corrosion process and, therefore, biodegradability of the implant is not advisable. Hence, recent investigation has focused on the development of metallic materials that are at once biodegradable and biocompatible with the elasticity near human bone. The rate of degradation by corrosion of biocompatible alloys can be controlled by surface improvement or thermal and mechanical treatment. The aim of this work was to prepare the new biodegradable alloy on the base of Mg-Ca-Zn-Mn and study the influence of thermomechanical treatment on the alloy microstructure, phase composition, microhardness and corrosion properties. Homogenization annealing was performed at 480 °C for 24 h followed by water quenching. The material was subjected to one pass of equal channel angular pressing (ECAP) at 290 °C. The microstructure study was performed for as-cast, heat-treated and ECAPed conditions and was accomplished by microhardness measurement. The chemical and phase composition was observed using of a scanning electron microscope and EDX analysis. To determine the corrosion properties of the alloy, an immersion test was performed together with the measurement of the potentiodynamic polarization.

Keywords: Biocompatible alloys, Mg alloy, ECAP, corrosion properties, heat treatment

1. INTRODUCTION

Magnesium alloys have attracted considerable attention, especially in the field of orthopedic and traumatology implants. The temporary implant must meet certain key attributes. Depending on the application, the requirements for the properties of the material can vary. However, if we focus primarily on temporary orthopedic and traumatology implants, then the most desirable properties include biocompatibility, adequate mechanical properties, natural degradability and osteogenesis. Convenient mechanical properties, low Young modulus and density of the Mg based alloys are closer to human bone than the properties of other metallic materials used in biomedicine. In addition, magnesium offers excellent biocompatibility, bioresorbability and biodegradability [1,2]. The Mg ion is a body metabolite contained in the bones and is absorbed daily in the range of 250 to 300 mg/day [3]. This ion is essential for bone cell growth and new bone formation. Although Mg based alloys are the most suitable biodegradable materials for medical implants, it is important to continue experimental research and improvement of their surface properties due to high susceptibility to corrosion and rapid degradation in the human body [4,5]. The reactivity of Mg leads to hydrogen gas formation and

accelerates the degradation resulting in low mechanical properties and possible implant failure before the healing time [1,6]. Microstructure refining, alloying, surface modification, machining, etc. can increase the mechanical properties and corrosion resistance of Mg based alloys. Various studies have shown that coating of the Mg material leads to increased corrosion resistance [2] and thus the requirements of controlled biodegradability is improved [7].

2. EXPERIMENT

The Mg–Ca–Zn–Mn-based alloy was prepared from pure Mg, Mg–Ca and Mg–Zn master alloys purchased from American Elements, USA, and pure Mn. The melting was carried out in a Leybold-Hereus 250 V/4KHz vacuum induction furnace with a maximum power input of 40 kW and a caisson volume of 104 l. However, as a result of the evaporation of Zn in vacuum, the alloy was melted in a protective argon atmosphere. The feed material, despite its high purity, contained very low concentrations of Fe, Cu, Ni and Si, which occurred in the form of poorly precipitated intermetallic phases.

The prepared ingot was heat treated in Linn HT1800 in flowing argon at 480 °C for 24 hours and water quenched. After homogenization treatment, 8x8x45 mm cuboidal samples of were worked and one pass of ECAP at 290 °C was performed.

Before observing the microstructure, the samples were metallographically prepared using the MTH APX 010 device. Grinding was performed by means of SiC papers of grain size up to P2500. DP-Mol cloth, DP-Lubricant Yellow and diamond DP-spray P with a particle size of 1 µm were used for polishing. The final polishing was carried out on DP-Nap cloth soaked in DP-Lubricant Yellow and diamond DP-spray P with a particle size of 0.25 µm. The specimens were etched by means of a solution composed of 10 ml H₂O, 70 ml ethanol, 10 ml acetic acid and 4.2 g picric acid. Grain boundaries were highlighted with a modified concentration of etching solution: 10 ml H₂O, 100 ml ethanol, 5 ml acetic acid and 6 g picric acid. The microstructure of the samples was observed using an OLYMPUS GX51 inverted metallographic microscope equipped with a digital camera. Phase analysis was performed by a JEOL JSM-6490LV scanning electron microscope equipped with an EDS probe (Oxford INCA x-act energy dispersion spectral). Both microstructure and phase analysis were examined for as-cast, thermal treated and ECAPed conditions.

To examine the influence of thermal and mechanical treatment on mechanical properties, Vickers microhardness measurement was performed using FUTURE-TECH FM-100 automatic microhardness tester with a control unit FM-ARS900. A total of 10 indentations with a predefined load of 50 g and a time of 10 s were made for each of the samples.

Table 1 Composition of artificial plasma used as the corrosive solution

| Compound | NaCl | CaCl ₂ | KCl | MgSO ₄ | NaHCO ₃ | Na ₂ HPO ₄ | NaH ₂ PO ₄ | H ₂ O |
|----------|------|-------------------|------|-------------------|--------------------|----------------------------------|----------------------------------|------------------|
| (g/l) | 6.80 | 0.20 | 0.40 | 0.10 | 2.20 | 0.126 | 0.026 | balance |

To determine the corrosion behavior of the alloy, potentiodynamic polarization was made using a three-electrode cell, an Autolab PGSTAT 128n apparatus and Nova 1.10 software. The surface of the specimen was ground with SiC papers of up to P2500 and then polarized from –1.9 V to -1.5 V with a scan rate of 1 mV/s in the solution of artificial plasma with composition summarized in **Table 1**. The solution temperature was 21.5 °C.

3. RESULTS AND DISCUSSION

3.1. Microstructural analysis

Figure 1 a) shows the microstructure in the longitudinal section of the as-cast ingot. The microstructure has a fine-grained and relatively homogeneous character. The average grain size is around 170 ± 87 µm. The

intermetallic phases are distributed mainly along the grain boundaries; few of them are located inside the grains. Local casting defects can also be found in the structure, especially pores, oxide films, or shrinkage cavities.

The microstructure in the longitudinal section of the ingot after thermal treatment is shown in **Figure 1 b)**. It is obvious that the homogenization annealing led to the microstructure being different from that of the as-cast condition. After heat treatment, the microstructure shows a clearly coarse-grained character with grains reaching about $291 \pm 64 \mu\text{m}$ in average size. Similarly, as in the as-cast condition, a considerable amount of porosity can be observed. Thermal treatment allowed the dissolution of some intermetallic phases located along the grain boundaries and their precipitation within the grains.

During one pass of the ECAP process the grains in the microstructure were refined and also elongated in the direction of deformation, as it is present in **Figure 1 c)** for the longitudinal section of the sample. Shear bands, subgrains and new recrystallized grains that are related to dynamic recovery and dynamic recrystallization were also observed. The average grain size reaches $96 \pm 107 \mu\text{m}$. As **Figure 1 c)** shows, casting defects are still present and have not been eliminated by the ECAP process as expected.

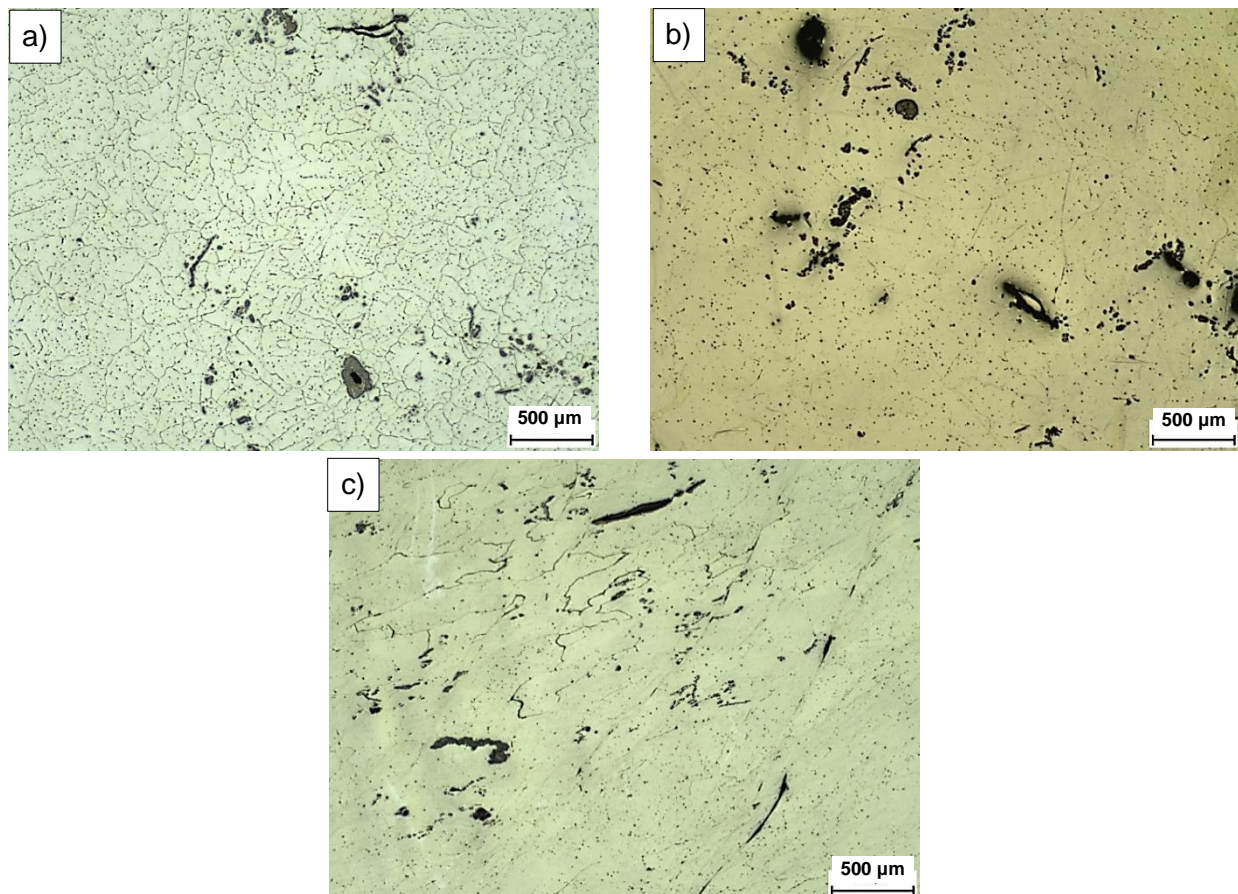


Figure 1 Optical micrographs of the microstructure of the samples under various conditions: **a)** as-cast, **b)** thermal treated, **c)** ECAPed

3.2. Phase analysis

The composition of the alloy was analyzed in as-cast and heat-treated condition and it was stated that the Mg-0.4Ca-1.0Zn-0.8Mn alloy (in wt%) was prepared. **Figure 2** shows the SEM microstructure of the ingot in as-cast and thermal treated condition with a detailed view of the intermetallic phase particles. EDS analysis of

both conditions showed a Mn content of about 0.8 wt%. The exact composition of the phases observed in the matrix, which were on the bases of Mg-Ca-Zn, Mg-Ca-Zn-Mn-Ni and Mg-Ca-Zn-Mn-Ni-Si has not been determined. After thermal treatment, some phases dissolved and Mn was redistributed in other phases. By comparing the microstructures in **Figure 2** it is evident that due to homogenization of the alloy during 24 hours of annealing, some phases along the grain boundaries dissolved and subsequently precipitated within the grains.

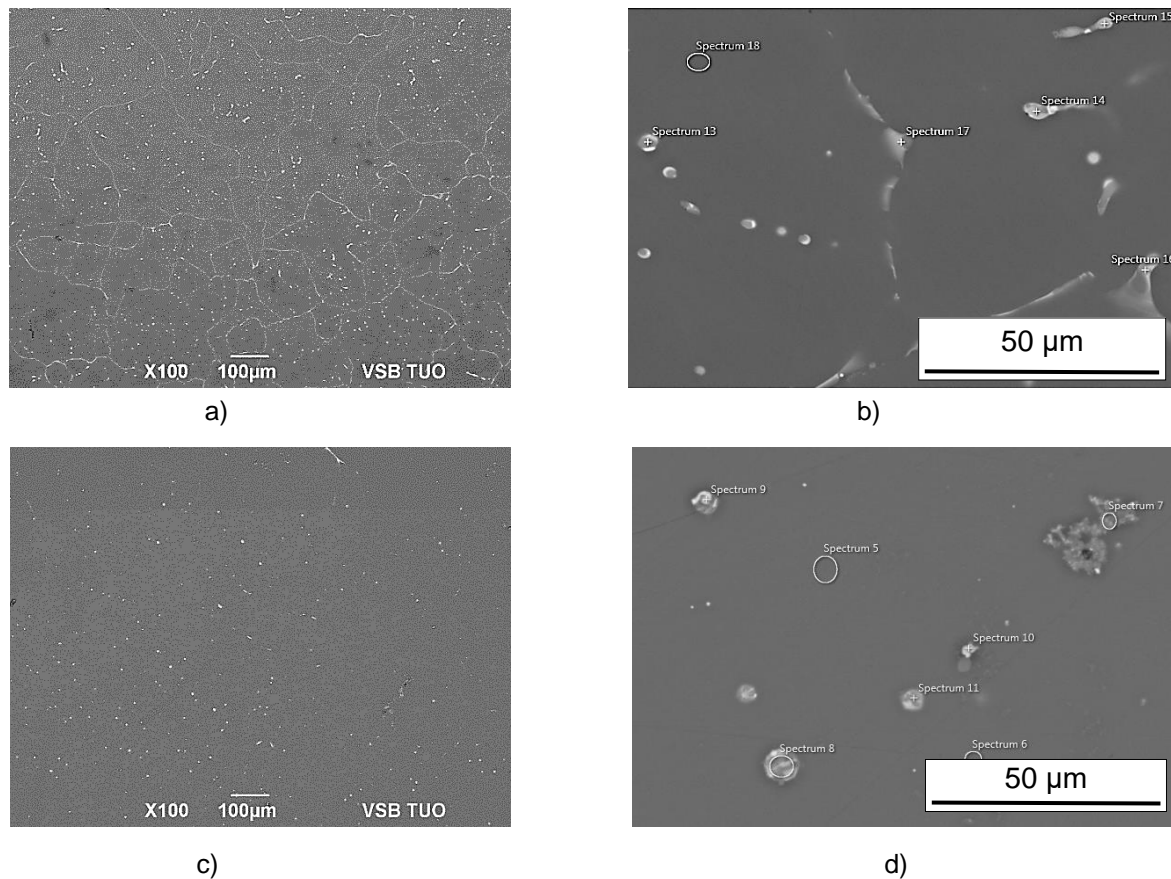


Figure 2 SEM micrograph of the alloy: a) grain boundaries with precipitates in as-cast condition, b) details of phases precipitated in as-cast sample, c) effect of thermal treatment on dissolution and redistribution of precipitates, d) details of secondary phases in the thermal treated sample

3.3. Microhardness measurement

The Mg based alloy is a soft material comparing Ti or Ni alloys, so the measurement of microhardness at a load of 100 g was incorrect due to the formation of very large indentations upon loading. For this reason, the measurement at a load of 50 g was preferred.

Table 2 Hardness values HV0.05 for samples under various thermal and mechanical conditions

| Sample | Microhardness |
|-----------------|---------------|
| | HV0.05 |
| As-cast | 52 ± 3 |
| Thermal treated | 59 ± 5 |
| ECAPed | 73 ± 5 |

The lowest microhardness HV0.05 was measured for the sample in the as-cast condition. Thermal treatment led to dissolution and/or more homogeneous distribution of precipitates which resulted in a higher microhardness. As expected, after ECAP, the microhardness values were the highest due to plastic deformation, internal stresses, and grains refinement. The microhardness values are summarized in **Table 2**.

3.4. Corrosion behavior

The corrosion resistance of the specimens was dependent on the thermal and mechanical conditions. The corrosion rate, corrosion potential, polarization resistance, and other parameters determined by the Tafel analysis are summarized in **Table 3**.

Table 3 Measured values from Tafel analysis

| Sample | Corrosion rate v_{corr} (mm/year) | Corrosion potential E_{corr} - Calc (V) | Corrosion potential E_{corr} - Obs (V) | Corrosion current density j_{corr} ($\mu\text{A}/\text{cm}^2$) | Polarization resistance R_{corr} (Ω) | Corrosion current (μA) |
|-----------------|-------------------------------------|---|--|--|---|-------------------------------------|
| Thermal treated | 9.9 | -1.77 | -1.67 | 216.1 | 249.8 | 410.6 |
| ECAPed | 6.6 | -1.64 | -1.65 | 156.5 | 416.9 | 244.1 |

After thermal treatment, the sample has a higher corrosion rate of 9.9 mm/year and the most negative corrosion potential value of -1.67 V compared to the ECAPed sample. On the contrary, the ECAPed sample appears to be more resistant with a lower corrosion rate of 6.6 mm/year. It is evident that annealing is not sufficient to improve the corrosion resistance of the Mg-0.4Ca-1.0Zn-0.8Mn alloy and ECAP treatment is needed for better corrosion behavior in artificial plasma solution.

4. CONCLUSION

From metallographic observations, it can be concluded that the as-cast samples contained considerable porosity and casting defects. The occurrence of the phases based on Mg-Ca-Zn, Mg-Ca-Zn-Mn-Ni and Mg-Ca-Zn-Mn-Ni-Si and located along the grain boundaries was determined from the phase analysis.

After thermal treatment, the grain size increased and the intermetallic particles were dissolved and subsequently redistributed inside the grains. The ECAP method elongated the grains in the extrusion direction and affected the decrease in grain size.

The highest microhardness values were reached for the sample after ECAP, as expected. In comparison to the as-cast state, after thermal treatment, the microhardness increased due to the more homogeneous distribution of precipitates in the grains.

From the measurement of potentiodynamic polarization and Tafel analysis, it can be seen that the sample after ECAP showed the lowest corrosion rate. This proves that only heat treatment does not have a sufficient effect on increasing corrosion resistance.

ACKNOWLEDGEMENTS

This work has been realized in the framework of the following projects: NU20-08-00150 "Biodegradable magnesium-based implants with tailored microstructure and defined degradation rate", as well as within the projects SGS SP2022/68" Specific Research in the Metallurgical, Materials and Process Engineering" and SGS SP2022/65" Materials based on non-ferrous metals — preparation, processes for improving their properties, area of application and the possibilities of recycling selected types of waste ".

REFERENCES

- [1] MINÁRIK, P., KRÁL, R., JANEČEK, M. Effect of ECAP processing on corrosion resistance of AE21 and AE42 magnesium alloys. *Applied Surface Science* [online]. 2013, vol. 281, pp. 44-48 [cit. 2022-05-05]. ISSN 0169-4332. Available from: <https://doi.org/10.1016/j.apsusc.2012.12.096>
- [2] KNAPEK, Michal, ZEMKOVÁ, Mária, GREŠ, Adam, JABLONSKÁ, Eva, LUKÁČ, František, KRÁL, Robert, BOHLEN, Jan, MINÁRIK, Peter. Corrosion and mechanical properties of a novel biomedical WN43 magnesium alloy prepared by spark plasma sintering. *Journal of Magnesium and Alloys* [online]. 2021, vol. 9, no. 3, pp. 853-865 [cit. 2022-05-05]. ISSN 2213-9567. Available from: <https://doi.org/10.1016/j.jma.2020.12.017>
- [3] KUMAR, Rajender, KATYAL, Puneet. Effects of alloying elements on performance of biodegradable magnesium alloy. *Materials Today: Proceedings* [online]. 2022, vol. 56, pp. 2443-2450 [cit. 2022-05-05]. ISSN 2214-7853. Available from: <https://doi.org/10.1016/j.matpr.2021.08.233>
- [4] GUNGOR, A., INCESU, A. Effects of alloying elements and thermomechanical process on the mechanical and corrosion properties of biodegradable Mg alloys. *Journal of Magnesium and Alloys* [online]. 2021, vol. 9, no. 1, pp. 241-253 [cit. 2022-05-05]. ISSN 22139567. Available from: <https://doi.org/10.1016/j.jma.2020.09.009>
- [5] BAIRAGI, Darothi, MANDAL, Sumantra. A comprehensive review on biocompatible Mg-based alloys as temporary orthopaedic implants: Current status, challenges, and future prospects. *Journal of Magnesium and Alloys* [online]. 2022, vol. 10, no. 3, pp. 627-669 [cit. 2022-05-05]. ISSN 22139567. Available from: <https://doi.org/10.1016/j.jma.2021.09.005>
- [6] YANG, Y., SCENINI, F., CURIONI, M.. A study on magnesium corrosion by real-time imaging and electrochemical methods: relationship between local processes and hydrogen evolution. *Electrochimica Acta* [online]. 2016, vol. 198, pp. 74-184 [cit. 2022-05-15]. ISSN 00134686. Available from: <https://doi.org/10.1016/j.electacta.2016.03.043>.
- [7] KIRKLAND, N.T., BIRBILIS, N., STAIGER, M.P. Assessing the corrosion of biodegradable magnesium implants: A critical review of current methodologies and their limitations. *Acta Biomaterialia* [online]. 2012, vol. 8, no. 3, pp. 925-936 [cit. 2022-05-15]. ISSN 17427061. Available from: <https://doi.org/10.1016/j.actbio.2011.11.014>